



Glass transition and rigidity in the aging linear harmonic oscillator model

Hugo M. Flores-Ruiz^{*,a}, Gerado G. Naumis^b, M. Micoulaut^c

^a Departamento de Ciencias Naturales y Exactas, CUValles, Universidad de Guadalajara, Carr. Guadalajara-Ameca km 45.5, 46600, Ameca, Jalisco, México

^b Depto. de Sistemas Complejos, Instituto de Física, Universidad Nacional Autónoma de México, Apdo. Postal 20-364, Mexico City 01000, Mexico

^c Sorbonne Universités, UPMC Université Paris 06, UMR 7600, LPTMC, F-75005 Paris, France

ARTICLE INFO

Keywords:

Glass transition

Rigidity

Fragility

Glass transition temperature

ABSTRACT

Rigidity theory in glasses was originally formulated to understand the relationship between network topology and glass forming ability, the later given by the minimal cooling rate required to form a glass. Here a study is presented on the glass transition temperature, specific heat and cooling/heating rate in a simple solvable low-temperature Monte Carlo Keating-like oscillator model. For a fixed heating rate, the results indicate that the glass transition temperature grows with the number of constraints as observed in real experiments. Moreover, to achieve glass transition, higher heating rates are needed as the number of constraints is decreased. These results are traced back to the high number of low-entropic energy barriers seen in flexible systems. Also, from the model, the fragility index is obtained and it shows an intermediate isostatically rigid phase which agrees, in a qualitatively level, with the experimental and computational evidence in some glasses.

1. Introduction

Glass transition is known to be a difficult problem due to its non-equilibrium character [1–3]. In spite of this, there are two aspects that everyone accept as fundamental: the glass forming ability (GFA) depends upon the relaxation times in the related supercooled liquid [4–7] and on the nucleation and crystallization kinetics [8].

There are many experimental and empirical rules to relate this GFA with chemical composition, network topology, bonding type, thermal and mechanical processes, etc. [7,9]. In chalcogenides, during the last 50 years there has been a systematic study of the GFA as a function of the network topology and chemical composition [7].

Rigidity theory (RT) has been proposed several years ago to relate the GFA and of the precursor alloy composition [10,11]. In this theory, covalent bonds are seen as mechanical constraints. Then a balance arises between degrees of freedom and constraints. When there are more degrees of freedom than constraints the system is called flexible (soft), and associated with this condition there are modes with low frequencies named floppy modes [12–14]. On the other hand, as the constraints increase the system is more rigid and the number of floppy modes decrease. When the number of freedom degrees is equal to constraints, there are no floppy modes and the system is isostatically rigid. When the number of constraints is bigger than the degrees of freedom the system is classified as stress rigid. RT has been corroborated experimentally on several chalcogenides glasses [4,15–17]. For

instance, recent experimental studies found that the main contribution to low frequency modes in AsS glasses is due to soft and rigid nanoclusters immersed in the bulk [16]. Also, according to RT and the experimental evidence, rigid networks are better glass forming [4]. Along the time, theory and computational models have been proposed to connect RT concepts and GFA [18–24]. In connection with RT, an intermediate isostatically rigid phase (IP) arises in several glasses [25]. This phase is a gap between the flexible and stress rigid regions and is characterized for being stress free. As a consequence, optical, mechanical, electrical and thermal unique properties are presented in glasses along the IP. For instance, properties from the molten alloys like diffusion, viscosity, non reversing heat flow, etc. show a minimum, maximum or constant behaviour in the IP [7,15,19,26,27].

One important parameter in the glass forming is the glass transition temperature (T_g). Several definitions of T_g are found in the literature, for instance, on cooling T_g is defined as the temperature at which the viscosity of a melt reaches 10^{12} Pa · s [28]. In contrast, during heating T_g is obtained from the inflection point in the heat flow [26,27]. The heating or cooling can be done by linear or modulated differential scanning calorimetry (DSC or MDSC respectively) [29–32]. The evidence shows that T_g depends on chemical composition (constraints concentration) of the glass, the cooling/heating rate, etc. Experiments show that T_g follows a growth tendency as constraints increase (the system goes from flexible to rigid) [4,27]. In this sense, theoretical efforts have been done in order to explain the connection between T_g , the

* Corresponding author.

E-mail address: hugo.flores@academicos.udg.mx (H.M. Flores-Ruiz).

chemical composition and rigidity [33–37]. As it was mentioned, T_g depends on the cooling/heating rate. The general tendency is that T_g grows as the heating speed is faster [38,39].

The fragility index is another important parameter to characterize the GFA on cooling. This index is proportional to the speed of change of the viscosity (in a logarithmic scale) with respect to the inverse temperature at T_g . According to Angell's classification, strong and fragile glasses may be defined [28]. In general, strong and fragile glassy materials show low and high values of fragility respectively. An interesting tendency arises when the fragility is analyzed from the RT perspective. In general it is observed that for several types of glasses, the fragility index show a minimum along the IP, i.e. for a certain glass alloys precursors, their fragility as function of composition goes from fragile to strong and then to fragile behaviour [7,15,19,26,27].

Contributions to modeling the glass forming by the cooling/heating process are found in the literature. Some of these efforts use a two level system to describe the glass forming dependence on cooling speed [40–42]. Others employ a Monte Carlo dynamics to study glassy systems [43,44] and the connection with RT [45]. Also, the relaxation time and enthalpy relaxation point of view has been used [46,47].

The present work tackles the glass forming and how is influenced by the rigidity and the cooling/heating speed by means of a solvable Monte Carlo Keating-like harmonic oscillator model. In order to achieve this, different quantities are analysed like heat capacity, glass transition temperature, energy of the system and fragility index.

The paper is organized as follows. In Section 2 the model is developed. In Section 3 the results are shown and finally in Section 5 the conclusions are given. In Appendix A, an implicit relationship between T_g , constraints and heating rate is proposed, and finally in Appendix B an expression for the fragility index is given in terms of constraints and T_g .

2. The model

We consider a network of N atoms with mass m in 3 dimensions. This network can be seen as a set of $3N$ oscillators in the normal mode space. Let's suppose that we have two types of oscillators. On the one hand, a density of modes, f , with frequency ω , associated with local distortions of the network with a low cost in energy, also called floppy modes; and on the other hand, a density of oscillators, n_c , with frequency Ω , related with the constraints imposed by bond-bending (BB) and bond-stretching (BS) forces. The energy of these $3N$ oscillators in the harmonic approach is [21]:

$$V = \frac{m\omega^2}{2} \sum_{j=1}^{Nf} Q_j^2 + \frac{m\Omega^2}{2} \sum_{j=Nf+1}^{3N} Q_j^2, \quad (1)$$

where Q_j is the coordinates of the normal mode j . As the total number of modes is always $3N$ we have the following relationship,

$$n_c + f = 3 \quad (2)$$

with $0 \leq n_c \leq 3$. The frequency of the floppy modes, ω , can be related with Ω as $\omega = \gamma\Omega$, and in glasses usually $\gamma \approx 1/6$ [45].

Once the mechanical model is set, we study the cooperative dynamics that results by cooling and heating the system. In order to do that, we follow the Ritort et al. [43,44] model. Within such approach, Ritort et al. are able to model glassy dynamics by means of a system of non-interacting harmonic oscillators evolving according to Monte-Carlo dynamics.

The method starts by using a Monte-Carlo procedure to relax the system. Within this approach, a new mechanical configuration Q_j' is made by adding a random displacement R_j ,

$$Q_j' = Q_j + R_j/\sqrt{3N} \quad (3)$$

where R_j follows a Gaussian distribution with zero mean and variance

Δ^2 . This new configuration with energy, V' , implies a energetic cost $\Delta V = V' - V$ given by,

$$\Delta V = \frac{m\omega^2}{2} \sum_{j=1}^{Nf} \left[\frac{2Q_j R_j}{\sqrt{3N}} + \frac{R_j^2}{3N} \right] + \frac{m\Omega^2}{2} \sum_{j=Nf+1}^{3N} \left[\frac{2Q_j R_j}{\sqrt{3N}} + \frac{R_j^2}{3N} \right]. \quad (4)$$

According to the Metropolis algorithm [48], the new configuration will be accepted with probability 1 if $\Delta V \leq 0$ and with probability $\exp(-\beta\Delta V)$ if $\Delta V > 0$. Following the Monte-Carlo procedure, ΔV must follow a probability distribution given by,

$$P(\Delta V) = \int_{-\infty}^{\infty} \dots \int_{-\infty}^{\infty} \prod_{j=1}^{3N} \frac{1}{\sqrt{2\pi\Delta^2}} \exp\left(-\frac{R_j^2}{2\Delta^2}\right) \times \delta\left[\Delta V - \frac{m\omega^2}{2} \sum_{j=1}^{Nf} \left(\frac{2Q_j R_j}{\sqrt{3N}} + \frac{R_j^2}{3N}\right) - \frac{m\Omega^2}{2} \sum_{j=Nf+1}^{3N} \left(\frac{2Q_j R_j}{\sqrt{3N}} + \frac{R_j^2}{3N}\right) dR_j\right]. \quad (5)$$

If the Dirac's delta function is used in an integral form and the Gaussian integrals are performed, Eq. (5) can be rewritten like,

$$P(\Delta V) = \frac{1}{2\sqrt{\pi X(t)}} \exp\left[-\frac{(\Delta V - V_0)^2}{4X(t)}\right], \quad (6)$$

where

$$V_0 = \frac{m\Delta^2}{2} (f\omega^2 + n_c\Omega^2) \quad (7)$$

and

$$X(t) = m\Delta^2 (f\omega^2\langle e(t) \rangle + n_c\Omega^2\langle E(t) \rangle), \quad (8)$$

with

$$\langle e(t) \rangle = \frac{m\omega^2}{2} \langle Q^2 \rangle \quad (9)$$

$$\langle E(t) \rangle = \frac{m\Omega^2}{2} \langle Q^2 \rangle. \quad (10)$$

In Eqs. (8), (9) and (10), t represents time and the brackets an average over initial conditions and dynamical trajectories of the system. From the Metropolis rule, the evolution of the energy, V , as function of time t is given by

$$\tau_0 \frac{\partial V}{\partial t} = \int_{-\infty}^0 xP(x)dx + \int_0^{\infty} xP(x)e^{-\beta x}dx \quad (11)$$

with $x = \Delta V$, $\beta = 1/k_B T$, T the temperature, k_B the Boltzmann's constant, and τ_0 a typical time during which ΔV has been performed. When the probability distribution given by Eq. (6) is inserted in Eq. (11), it leads to

$$\tau_0 \frac{\partial V}{\partial t} = \frac{V_0}{2} \left[\left(1 - \frac{2\beta X(t)}{V_0}\right) g(t) + \text{Erfc}\left(\frac{V_0}{2\sqrt{X(t)}}\right) \right], \quad (12)$$

with Erfc the complementary error function and

$$g(t) = \exp(-\beta V_0 + \beta^2 X(t)) \text{Erfc}\left(\frac{2\beta X(t) - V_0}{2\sqrt{X(t)}}\right). \quad (13)$$

It is important to notice that Eq. (12) is not closed because it depends on $X(t)$, and $X(t)$ turns out to depend on $\langle e(t) \rangle$ and $\langle E(t) \rangle$. In order to have a closed form of Eq. (12), an adiabatic approximation can be implemented [44]. The adiabatic approximation becomes asymptotically valid for enough long times. In this approach $X(t)$ is related with $V(t)$ assuming that the system has been partially equilibrated at energy $V(t)$, namely,

$$X(t) = 2V_0 V(t). \quad (14)$$

Under condition (14), the Eq. (12) can be solved as function of time, of course, one keeps in mind that the temperature T depends on time t .

On the other hand, the heat capacity $C(T)$ is the variation of the energy V respect to the temperature T . A natural relation arises between Eq. (12) and $C(T)$,

$$C(T) = \frac{\partial V}{\partial T} = \frac{\partial V}{\partial t} \frac{1}{\dot{T}} \quad (15)$$

where $\dot{T} = dT/dt$ is proportional to the cooling/heating rate. If Eq. (12) is solved as function of t , the energy V can be seen as function of T due to Eq. (15).

Finally, the equilibrium solution of Eq. (12) at high temperatures is [44]

$$V_{eq}(T) = \frac{T}{2}, \quad (16)$$

in concordance with the equipartition theorem.

3. Results

As mentioned before, we are interested in the influence of n_c on glass forming. To achieve that, several cooling/heating cycles were performed and quantities like $V(T)$, $C(T)$ and T_g were obtained. To do so, the Eq. (12) was numerically solved using the relation (14). A linear dependence of the temperature with time was used,

$$T(t) = T_i \pm qt, \quad (17)$$

with T_i the initial temperature and q the magnitude of the cooling/heating rate. In Eq. (17), the signs - and + were used when the system is cooled or heated respectively.

To evaluate V_0 in Eq. (7), values for m , Δ and Ω were assigned and fixed in all results using units where the Boltzmann's constant is $k_B = 1$ and $\tau_0 = 1$. Here we used $m = 1$, $\Delta = 0.4$, $\Omega = 0.2$ and $\omega = \Omega/6$. The free parameters in V_0 are the density of floppy modes f and the density of constraints n_c , both related by $f = 3 - n_c$. Once V_0 is parameterized, we simulated the cooling of the oscillators by means of solving Eq. (12) from a high temperatures T_0 to a low temperature T_l . The initial energy at T_0 is given by assuming thermal equilibrium $V_1 = T_0/2$. T_0 goes to T_l according to Eq. (17), therefore a cooling rate was set. To perform the heating, the final temperature and final energy of the cooling were the initial temperature and initial energy of the heating in Eq. (12).

Fig. 1 shows the resulting normalized energy $V(T)/V_1$ evolution as a function of the normalized temperature T/T_0 for different constraint numbers and by fixing the cooling/heating rate at $q = 0.0001$. In the same

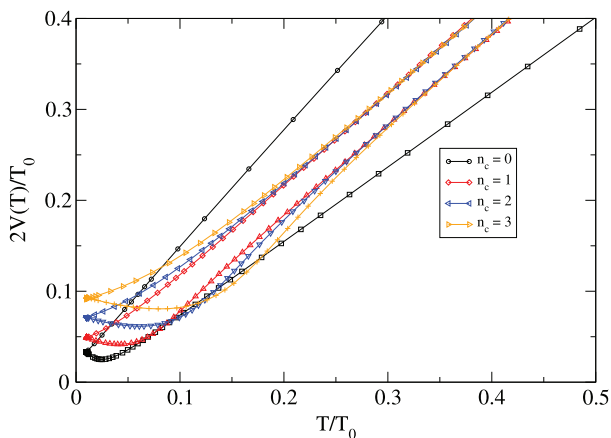


Fig. 1. Normalized energy $V(T)/V_1$ as a function of the normalized temperature T/T_0 for different constraint number with a fixed cooling/heating rate of $q = 0.0001$. For a fixed constraint number, the upper curve corresponds to the cooling while the lower is the heating. Notice the hysteresis of the cycles, which is specially prominent for the most flexible system $n_c = 0$.

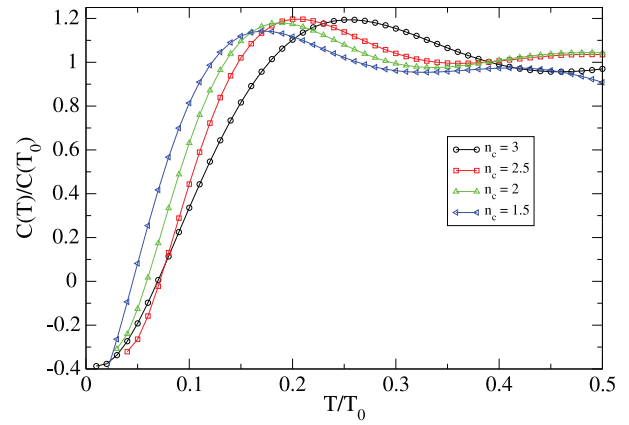


Fig. 2. Normalized heat capacity $C(T)/C(T_0)$ as a function of the normalized temperature T/T_0 , for different constraint number with a fixed heating rate of $q = 0.0001$. The inflexion point in the jump corresponds to T_g . Observe how T_g grows with n_c , in agreement with many observational trends.

figure, we observe a glassy behaviour at low temperatures as $V(T)/V_1$ deviates from its equilibrium value $V_{eq} = T/2$ (see Eq. (16)). From Fig. 1, one notices that as n_c increases, the systems are more rigid and their energies at the end of the cooling are higher. For example, the system with $n_c = 0$ ($f = 3$) departs more from equilibrium in the cooling/heating process and its final energy in the cooling is the lowest. In contrast, for $n_c = 3$ ($f = 0$) the system is more rigid and its final energy during the cooling is higher than the rest of the systems. The previous observations are in qualitative agreement with the experimental evidence, as flexible systems are related with fragile glasses and rigid systems with strong glasses in general [4,27].

According to Eq. (15), the heat capacity $C(T)$ can be determined from the curves presented in Fig. 1. Fig. 2 shows the evolution of $C(T)$ normalized by the heat capacity at high temperature $C(T_0)$ for different constraints at a fixed heating rate $q = 0.0001$.

An experimental procedure to measure the glass transition temperature T_g is to look for the inflection point in the heat flow or heat capacity [4,26]. We follow the same procedure to extract T_g from $C(T)$ (see Eq. (15)), i.e., during heating we find the inflection point at low temperatures (see Fig. 2). Fig. 3 presents T_g normalized by T_0 as function of n_c . One notices that T_g increases as the system is more rigid which is in agreement with observational trends [4,26,27,35–37]. If the system is more flexible ($n_c < 1.5$), it is difficult to identify T_g because the inflection point in the heat capacity is not well defined at low

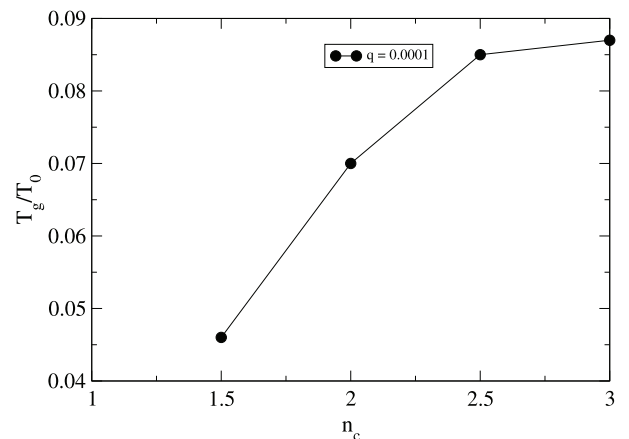


Fig. 3. Glass transition temperature T_g , normalized by T_0 , as a function of rigidity for a fixed heating rate of $q = 0.0001$, only for $n_c \geq 1.5$ it was possible to identify a defined T_g . Lower values require higher-heating speeds.

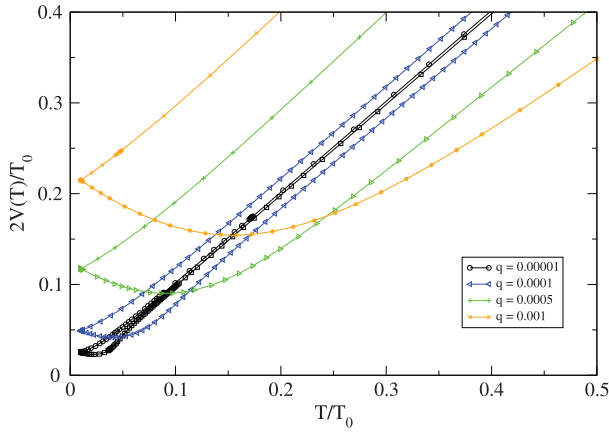


Fig. 4. Normalized energy $2V(T)/T_0$ as a function of the normalized temperature T/T_0 for a fixed constraint number $n_c = 1$, but with different cooling/heating rate. For a fixed cooling/heating speed, the upper curve corresponds to the cooling while the lower is the heating. The hysteresis and energy is reduced by slowing the cooling/heating. Eventually, T_g can not be defined according as the inflection point in $C(T)$ disappears.

temperatures. One solution to this issue is to increase the heating speed to push T_g at higher temperatures.

Fig. 4 presents the energy $V(T)$ normalized by the energy at high temperatures $V_1 = T_0/2$ as a function of T/T_0 , for $n_c = 1$ and different cooling/heating speeds. The glassy behaviour is present in all systems at low temperatures. This phenomenon is amplified with the use of higher cooling/heating rates, in fact, this trend has as a consequence that the energy is bigger at the end of the cooling.

As it was mentioned before, the heat capacity can be obtained from $V(T)$ through the relation (15). **Fig. 5** shows $C(T)/C(T_0)$ as a function of T/T_0 for a fixed constraint number $n_c = 2$ and different heating speeds. We observe that $C(T)/C(T_0)$ is well defined for low and intermediate heating rates, however, for higher ones $C(T)/C(T_0)$ behaves in a different way. One natural consequence of this tendency is the difficulty in finding T_g from the inflection point in $C(T)$, although one can always increase the cooling rate to obtain a readable T_g .

The fragility index is an important parameter in glass forming as is related with the liquid precursor ability to form a glass on cooling. According to Angell's fragility classifications [28], there are two types of glasses, strong and fragile. The fragility index M can be found in the presented analytical model when the system is heated. As shown in Appendix B, M is given by,

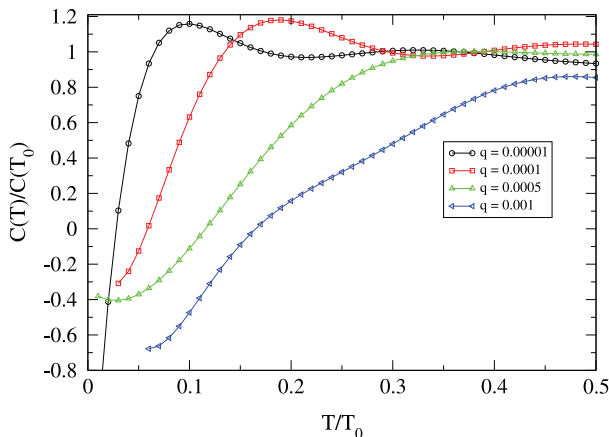


Fig. 5. Normalized heat capacity $C(T)/C(T_0)$ as a function of the normalized temperature T/T_0 for different heating rates with a fix constraint number $n_c = 2$. Observe that for the highest heating rate it is no longer possible to define a T_g .

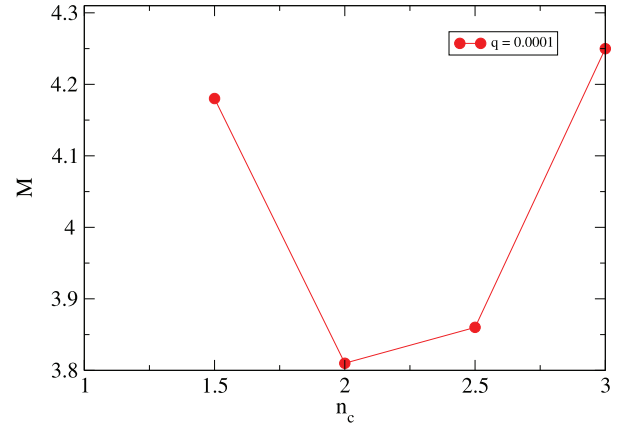


Fig. 6. Fragility index M as function of rigidity for the fixed heating rate $q = 0.0001$. Observe that M presents a minimum as the system goes from flexible ($n_c = 1.5$ or $f = 1.5$) to rigid ($n_c = 3$ or $f = 0$). The tendency of M qualitatively agrees with the experimental and simulated behaviour of the fragility index along the isostatically rigid intermediate phase of some chalcogenides melts [7].

$$M = \frac{3}{2} + \frac{V_0}{4T_g}, \quad (18)$$

where V_0 is given by Eq. (7) and T_g is the glass transition temperature.

Although in Eq. (18) we have $M = M(V_0, T_g)$, it turns out that $V_0 = V_0(f, n_c)$ and $T_g = T_g(f, n_c, \dot{T})$. Thus, we conclude that M depends on the density of constraints n_c , floppy modes f and the heating rate \dot{T} .

Fig. 6 shows the fragility index M (see Eq. (18)) as a function of n_c at a fixed heating rate $q = 0.0001$. M presents a minimum when the system goes to flexible ($n_c = 1.5$ or $f = 1.5$) from rigid ($n_c = 3$ or $f = 0$). M decreases from $n_c = 1.5$ to $n_c = 2.0$ and then it increases up to $n_c = 3$. This behaviour is similar to the isostatically rigid intermediate phase that present some chalcogenide melts when such a systems goes to flexible to rigid [7]. Low and high M values are related with strong and fragile glasses respectively. In our model, strong glasses are represented for low values of M when $n_c = 2.0$ and $n_c = 2.5$, and fragile glasses for high values of M when $n_c = 1.5$ and $n_c = 3$.

4. Discussion

From the previous results, is clear that $C(T)$, T_g and M are constraint and cooling/heating ratio dependent quantities as seen in experiments. The advantage of the present model is that allows to isolate in detail the nature of such effects. To see why these effects happen, in the Appendix A we show that according to Eq. (A.15), T_g is given by an implicit function of the density of constraints n_c , floppy modes f and the heating rate \dot{T} . These results are basically due to the constraint dependent relaxation time. As shown in Appendix B, near T_g the relaxation time has the form $\tau = \tau_0 \sqrt{\pi} \exp[E_A/4T]/2$ where $E_A = 12T \log(V_0/T) + V_0$. By using the definition of V_0 given Eq. (7), we obtain that,

$$V_0 = \frac{m\Delta^2\Omega^2}{2}(3 + (1 - \gamma^2)n_c) \quad (19)$$

As V_0 is a measure of the entropy barriers, we see that such barriers increase as n_c grows, in agreement with previous analysis of experimental data [21,35]. From this result, one obtains Eq. (18), which relates M with f and T_g .

It is interesting to compare the present results with those obtained from the temperature-dependent constraint theory, which started with early work by Gupta and Mauro [49–51] and eventually evolved into a new and highly accurate viscosity model known as the Mauro-Yue-El-lison-Gupta-Allison Model (MYEGA) [52,53]. This model allows to understand the chemical composition and temperature effects on the viscosity of glass-former melts [52,54,55]. In the temperature-

dependent constraint theory, fragility and glass transition temperature are shown to be dependent on constraints, which are activated by the temperature. To calculate the fragility, a relationship is invoked between the constraints and entropy. Such results are akin to those presented in this work, as we found here that entropy barriers are constraint and temperature dependent.

5. Conclusions

We presented the effects on the specific heat, glass transition temperature, energy hysteresis cycle and fragility index of a simple aging linear oscillator model in which constraints and floppy modes are included. The results reproduce the trends observed in experiments with some chalcogenide glasses, i.e., as the constraints are increased, T_g grows and the specific heat is modified. The glass forming tendency, measured by the cooling speed ratio to observe the glass transition, is also constraint dependent. The fragility index is also dependent on the rigidity and shows a minimum around the rigidity transition as observed in real glasses.

We ascribe all these effects to modifications in the height of the

Appendix A

In this Appendix A, an approach is presented at low temperatures to find out T_g on heating using the harmonic model (see Section 2). As a natural consequence T_g will be related with n_c and the heating rate in concordance with experimental evidence.

T_g is obtained by finding out the inflection point in $C(T)$ during heating. In order to do that, low temperatures ($\beta \rightarrow \infty$), the adiabatic approach (relation (14)) and long time limit ($V \rightarrow 0$) are considered. In the adiabatic approach, the evolution of the energy $V(t)$ given by Eq. (12) is rewritten as,

$$\tau_0 \frac{\partial V}{\partial t} = \frac{V_0}{2} \left[(1 - 4\beta V_0 V) g_1(t) + \text{Erfc} \left(\sqrt{\frac{V_0}{8V}} \right) \right], \quad (\text{A.1})$$

where

$$g_1(t) = \exp(-\beta V_0 + \beta^2 2V_0 V) \text{Erfc} \left(\sqrt{\frac{V_0}{8V}} (4\beta V - 1) \right). \quad (\text{A.2})$$

At low temperatures and in the long time limit, $\sqrt{\frac{V_0}{8V}} \rightarrow \infty$ and $\sqrt{\frac{V_0}{8V}} (4\beta V - 1) \rightarrow \infty$, then the complementary error functions in the Eqs. (A.1) and (A.2) can be expanded up to first order, in a generic way, like

$$\text{Erfc}(x) \approx \frac{\exp(-x^2)}{\sqrt{\pi}x} \left(1 - \frac{1}{2x^2} \right) \quad (\text{A.3})$$

with $x = \sqrt{\frac{V_0}{8V}}$ or $x = \sqrt{\frac{V_0}{8V}} (4\beta V - 1)$ respectively. Finally, from previous results the Eq. (A.1) is transformed to

$$\tau_0 \frac{\partial V}{\partial t} \approx \sqrt{\frac{32}{\pi V_0}} V^{3/2} \left[\frac{1}{(1 - 4\beta V)^2} - 1 \right] \exp(-V_0/8V). \quad (\text{A.4})$$

Using the Eq. (15) and the approach (A.4), the heat capacity $C(T)$ can be expressed as

$$C(T) \approx \frac{1}{\tau_0 T} \sqrt{\frac{32}{\pi V_0}} V^{3/2} \exp(-V_0/8V) \left[\frac{1}{(1 - 4\beta V)^2} - 1 \right]. \quad (\text{A.5})$$

To find out the inflection point of $C(T)$ at low temperatures, the first and the second derivative of $C(T)$ are needed, because the inflection point is a maximum in $\partial C(T)/\partial T$ and such a maximum is localized at T_g when $\partial^2 C(T)/\partial T^2 = 0$.

The first derivative of Eq. (A.5) is

$$\frac{\partial C(T)}{\partial T} = C(T) \left\{ \frac{C(T)}{V(T)} \left[\frac{3}{2} + \frac{V_0}{8V(T)} + G(T) \right] - \beta G(T) \right\}, \quad (\text{A.6})$$

where

$$G(T) = \frac{1}{(1 - 4\beta V(T))(1 - 2\beta V(T))}, \quad (\text{A.7})$$

and the second derivative is the following,

entropy barriers which are fully responsible for the system dynamics. Although in real glasses both energy and entropy play a role, the fact that experiments follow the trend observed here suggest that at least for systems below the rigidity transition, entropy produced by floppy modes is the main driving force behind the observed trends.

Declaration of Competing Interest

The authors declare that they have no known competing financial interests or personal relationships that could have appeared to influence the work reported in this paper.

Acknowledgments

We thank DGAPA-UNAM project IN106620. H.M.Flores-Ruiz gratefully acknowledges the computing time granted by LANCAD and CONACYT on the supercomputer Yoltla/Miztli/Xiuhcoatl at LSPV UAM-Iztapalapa/ DGTIC UNAM/ CGSTIC CINVESTAV.

$$\begin{aligned} \frac{\partial^2 C(T)}{\partial T^2} &= \frac{C(T)^3}{V^2} \left[2 \left(\frac{3}{2} + \frac{V_0}{8V} + G(T) \right)^2 - \left(\frac{3}{2} + \frac{V_0}{4V} + G(T) \right) \right] \\ &\quad - \frac{3C(T)^2}{V} \left(\frac{3}{2} + \frac{V_0}{8V} + G(T) \right) \beta G(T) \\ &\quad + \frac{2\beta C(T)}{V} (C - \beta V)^2 (3 - 8\beta V) G^2(T) \\ &\quad + \beta^2 C(T) G(T) (G(T) + 1). \end{aligned} \quad (\text{A.8})$$

From the condition $\partial^2 C(T)/\partial T^2 = 0$ imposed in Eq. (A.8), the following couple of equations are obtained,

$$C(T) = 0, \quad (\text{A.9})$$

and

$$\begin{aligned} \frac{C(T)^2}{V^2} \left[2 \left(\frac{3}{2} + \frac{V_0}{8V} + G(T) \right)^2 - \left(\frac{3}{2} + \frac{V_0}{4V} + G(T) \right) + 2\beta V (3 - 8\beta V) G^2(T) \right] \\ - \frac{C(T)}{V} \left[\left(\frac{3}{2} + \frac{V_0}{8V} + G(T) \right) 3\beta G(T) + 4\beta^2 V (3 - 8\beta V) G^2(T) \right] \\ + 2\beta^3 V (3 - 8\beta V) G^2(T) + \beta^2 G(T) (G(T) + 1) = 0, \end{aligned} \quad (\text{A.10})$$

where $G(T)$ is given by Eq. (A.7).

The Eq. (A.9) is satisfied when $V(T) = T/2$ at low temperatures. Therefore, T_g can be approximated as the temperature an intersection between $V(T)$ and $T/2$ at which occurs [45].

On the other hand, Eq. (A.10) can be worked out in the following way.

$$\frac{C(T)^2}{V^2} (2G^2(T) - G(T)) - \frac{C(T)}{V} (3\beta G^2(T)) + \beta^2 G^2(T) = 0, \quad (\text{A.11})$$

where dominant terms appear around the inflection point. This last Eq. leads to the next couple of relationships,

$$G^2(T) = 0 \quad (\text{A.12})$$

and

$$\left(\frac{C(T)}{V} \right)^2 - \frac{3}{2T} \left(\frac{C(T)}{V} \right) + \frac{1}{2T^2} = 0. \quad (\text{A.13})$$

If the Eq. (A.12) is not satisfied due to the form of $G(T)$ (see Eq. (A.7)), then the relationship (A.13) could contain the root that corresponds to an inflection point in $C(T)$. Eq. (A.13) is solved by taking the factor $C(T)/V$ as the variable and the terms $3/2T$ and $1/2T^2$ as the coefficients. The corresponding solutions are

$$\left(\frac{C(T)}{V} \right)_\pm = \frac{3}{4T} \pm \frac{1}{4T}, \quad (\text{A.14})$$

where the right solution in this context corresponds to the positive sign. Then from Eq. (A.14), T_g is estimated at the temperature where $C(T)/V(T)$ is equal to $1/T$. If the explicit form of $C(T)$ (see Eq. (A.5)) is used, T_g could be seen as an implicit function of the rest of the parameters, given by

$$\frac{1}{\tau_0 \dot{T}} \sqrt{\frac{32}{\pi V_0}} V(T_g)^{1/2} e^{-V_0/8V(T_g)} \left[\frac{T_g^2}{[T_g - 4V(T_g)]^2} - 1 \right] = \frac{1}{T_g}. \quad (\text{A.15})$$

From Eq. (A.15) is clear that $T_g(\tau_0, \dot{T}, V_0(f, n_c))$ and thus T_g is a function of the density of constraints n_c , floppy modes f and the heating rate \dot{T} .

Appendix B

Fragility M is one way to quantify the ability of a system to form a glass. In this appendix we obtain M from the harmonic model (see Section 2). M results in a function of the rigidity and the glass transition temperature T_g .

When a linearization of the energy V is performed around the equilibrium solution V_{eq} (see Eq. (16)), a relaxation time τ is found [45]. In order to get this time, V is expanded like,

$$V = V_{eq} \left[1 + \frac{1}{2} \frac{(V - V_{eq})}{V_{eq}} \right]. \quad (\text{B.1})$$

If the relation (B.1) is introduced in Eq. (12) with the condition $\frac{(V - V_{eq})}{V_{eq}} < 1$, then

$$\frac{\partial V}{\partial t} = \frac{V_0}{\tau} \left[1 + \frac{(V - V_{eq})}{2V_{eq}} \right]^{3/2} e^{V_0(V - V_{eq})/16(V_{eq})^2} \left[\frac{1}{(1 + 2\beta(V - V_{eq}))^2} - 1 \right], \quad (\text{B.2})$$

with the relaxation time τ given by

$$\tau = \tau_0 \sqrt{\frac{\pi}{32} \left(\frac{V_0}{V^*} \right)^3} e^{V_0/4T} = \frac{\tau_0}{2} \sqrt{\pi \left(\frac{V_0}{T} \right)^3} e^{V_0/4T} = \frac{\tau_0 \sqrt{\pi}}{2} e^{E_A/4T}, \quad (\text{B.3})$$

where $E_A = 12T \log\left(\frac{V_0}{T}\right) + V_0$.

The fragility M is defined as

$$M = \left. \frac{\partial \log \eta}{\partial (T_g/T)} \right|_{T=T_g}, \quad (\text{B.4})$$

where η is the viscosity, however this quantity is proportional to the relaxation time τ . In this way, M can be obtained from Eq. (B.3) and (B.4) like,

$$M = \left. \frac{\partial \log \tau}{\partial (T_g/T)} \right|_{T=T_g} = \frac{3}{2} + \frac{V_0}{4T_g}. \quad (\text{B.5})$$

It is clear from the previous Eq. (B.5) that $M(V_0, T_g)$, however $V_0(f, n_c)$ and $T_g(\tau_0, \dot{T}, V_0(f, n_c))$ (see Eq. (A.15)). Then as a natural consequence of the model, the fragility M depends on the density of constraints n_c , the floppy modes f , and T_g .

References

- [1] I. Gutzow, J. Schmelzer, *The Vitreous State: Thermodynamics, Structure, Rheology, and Crystallization*, Springer-Verlag, Berlin, 1995.
- [2] K. Binder, W. Kob, *Glassy Materials and Disordered Solids: An Introduction to their Statistical Mechanics*, World Scientific, 2011.
- [3] E.D. Zanotto, J. Mauro, The glassy state of matter: its definition and ultimate fate, *J. Non Cryst. Solids* 471 (2017) 490–495, <https://doi.org/10.1016/j.jnoncrysol.2017.05.019>.
- [4] M. Tatsumisago, B.L. Halfpap, J.L. Green, S.M. Lindsay, C.A. Angell, Fragility of ge-as-se glass-forming liquids in relation to rigidity percolation, and the Kauzmann paradox, *Phys. Rev. Lett.* 64 (1990) 1549–1552, <https://doi.org/10.1103/PhysRevLett.64.1549>.
- [5] K. Ngai, *Relaxation and Diffusion in Complex Systems*, Springer Science & Business Media, 2011.
- [6] H.B. Yu, W.H. Wang, H.Y. Bai, K. Samwer, The β -relaxation in metallic glasses, *Natl. Sci. Rev.* 1 (3) (2014) 429–461.
- [7] P. Boolchand, M. Bauchy, M. Micoulaut, C. Yildirim, Topological phases of chalcogenide glasses encoded in the melt dynamics, *Phys. Status Solidi (B)* 255 (6) (2018) 1800027, <https://doi.org/10.1002/psb.201800027>.
- [8] E.D. Zanotto, D.R. Cassar, The race within supercooled liquids-relaxation versus crystallization, *J. Chem. Phys.* 149 (2) (2018) 024503, <https://doi.org/10.1063/1.5034091>.
- [9] Y. Liu, T. Fujita, D. Aji, M. Matsuura, M. Chen, Structural origins of Johari-Goldstein relaxation in a metallic glass, *Nat. Commun.* 5 (2014) 3238.
- [10] J. Phillips, Topology of covalent non-crystalline solids i: short-range order in chalcogenide alloys, *J. Non Cryst. Solids* 34 (2) (1979) 153–181, [https://doi.org/10.1016/0022-3093\(79\)90033-4](https://doi.org/10.1016/0022-3093(79)90033-4).
- [11] M. Thorpe, Continuous deformations in random networks, *J. Non Cryst. Solids* 57 (3) (1983) 355–370, [https://doi.org/10.1016/0022-3093\(83\)90424-6](https://doi.org/10.1016/0022-3093(83)90424-6). <http://www.sciencedirect.com/science/article/pii/0022309383904246>
- [12] H. He, M.F. Thorpe, Elastic properties of glasses, *Phys. Rev. Lett.* 54 (1985) 2107–2110, <https://doi.org/10.1103/PhysRevLett.54.2107>.
- [13] H.M. Flores-Ruiz, G.G. Naumis, Boson peak as a consequence of rigidity: aperturbation theory approach, *Phys. Rev. B* 83 (2011) 184204, <https://doi.org/10.1103/PhysRevB.83.184204>.
- [14] H.M. Flores-Ruiz, G.G. Naumis, The transverse nature of the boson peak: a rigidity theory approach, *Physica B* 418 (2013) 26–31, <https://doi.org/10.1016/j.physb.2013.02.041>. <http://www.sciencedirect.com/science/article/pii/S0921452613001257>
- [15] P. Boolchand, X. Feng, D. Selvanathan, W. Bresser, *Rigidity Transition in Chalcogenide Glasses*, Springer US, Boston, MA, 2002, pp. 279–295.
- [16] R. Holomb, P. Ihatolia, O. Mitsa, V. Mitsa, L. Himics, M. Veres, Modeling and first-principles calculation of low-frequency quasi-localized vibrations of soft and rigid As–S nanoclusters, *Appl. Nanosci.* 9 (5) (2019) 975–986, <https://doi.org/10.1007/s13204-018-00948-5>.
- [17] B.J. Nordell, T.D. Nguyen, A.N. Caruso, W.A. Lanford, P. Henry, H. Li, L.L. Ross, S.W. King, M.M. Paquette, Topological constraint theory analysis of rigidity transition in highly coordinate amorphous hydrogenated boron carbide, *Front. Mater.* 6 (2019) 264, <https://doi.org/10.3389/fmats.2019.00264>. <https://www.frontiersin.org/article/10.3389/fmats.2019.00264>
- [18] A. Huerta, G. Naumis, Relationship between glass transition and rigidity in a binary associative fluid, *Phys. Lett. A* 299 (5) (2002) 660–665, [https://doi.org/10.1016/S0375-9601\(02\)00519-4](https://doi.org/10.1016/S0375-9601(02)00519-4). <http://www.sciencedirect.com/science/article/pii/S0375960102005194>
- [19] M. Micoulaut, M. Bauchy, H. Flores-Ruiz, *Topological Constraints, Rigidity Transitions, and Anomalies in Molecular Networks*, Springer International Publishing, Cham, 2015, pp. 275–311. DOI:10.1007/978-3-319-15675-0_11
- [20] M. Micoulaut, J.C. Phillips, Rings and rigidity transitions in network glasses, *Phys. Rev. B* 67 (2003) 104204, <https://doi.org/10.1103/PhysRevB.67.104204>.
- [21] G.G. Naumis, Energy landscape and rigidity, *Phys. Rev. E* 71 (2005) 026114, <https://doi.org/10.1103/PhysRevE.71.026114>.
- [22] H.M. Flores-Ruiz, G.G. Naumis, J.C. Phillips, Heating through the glass transition: a rigidity approach to the boson peak, *Phys. Rev. B* 82 (2010) 214201, <https://doi.org/10.1103/PhysRevB.82.214201>.
- [23] H.M. Flores-Ruiz, G.G. Naumis, Excess of low frequency vibrational modes and glass transition: a molecular dynamics study for soft spheres at constant pressure, *J. Chem. Phys.* 131 (15) (2009) 154501, <https://doi.org/10.1063/1.3246805>.
- [24] S. Kumar, Nirjhar, Sakshi, A. Singh, Study of glass-forming ability and structural rigidity of Zn-modified (GeTe)_x(Sb₂Te₃)_{100-x} chalcogenide glassy alloys, *Phase Transit.* 93 (1) (2020) 183–196, <https://doi.org/10.1080/01411594.2019.1679367>.
- [25] P. Boolchand, D.G. Georgiev, B. Goodman, Discovery of the intermediate phase in chalcogenide glasses, *J. Optoelectron. Adv. Mater.* 3 (3) (2001) 703–720.
- [26] P. Chen, P. Boolchand, D.G. Georgiev, Long term aging of selenide glasses: evidence of sub-tg endotherms and pre-tg exotherms, *J. Phys.* 22 (6) (2010) 065104, <https://doi.org/10.1088/0953-8984/22/6/065104>.
- [27] D. Selvanathan, W.J. Bresser, P. Boolchand, Stiffness transitions in $\text{Si}_x\text{Se}_{1-x}$ glasses from raman scattering and temperature-modulated differential scanning calorimetry, *Phys. Rev. B* 61 (2000) 15061–15076, <https://doi.org/10.1103/PhysRevB.61.15061>.
- [28] C. Angell, Structural instability and relaxation in liquid and glassy phases near the fragile liquid limit, *J. Non Cryst. Solids* 102 (1) (1988) 205–221, [https://doi.org/10.1016/0022-3093\(88\)90133-0](https://doi.org/10.1016/0022-3093(88)90133-0). Proceedings of the Ninth University Conference on Glass Science
- [29] M. Reading, A. Luget, R. Wilson, Modulated differential scanning calorimetry, *Thermochim. Acta* 238 (1994) 295–307, [https://doi.org/10.1016/S0040-6031\(94\)85215-4](https://doi.org/10.1016/S0040-6031(94)85215-4). <http://www.sciencedirect.com/science/article/pii/S0040603194852154>
- [30] R. Riesen, G. Widmann, R. Truttman, Alternating thermal analysis techniques, *Thermochim. Acta* 272 (1996) 27–39, [https://doi.org/10.1016/0040-6031\(95\)02608-8](https://doi.org/10.1016/0040-6031(95)02608-8). Advances in International Thermal Sciences: Environment, Polymers, Energy and Techniques
- [31] E. Verdonck, K. Schaap, L.C. Thomas, A discussion of the principles and applications of modulated temperature dsc (mtdsc), *Int. J. Pharm.* 192 (1) (1999) 3–20, [https://doi.org/10.1016/S0378-5173\(99\)00267-7](https://doi.org/10.1016/S0378-5173(99)00267-7). <http://www.sciencedirect.com/science/article/pii/S0378517399002677>
- [32] C.A. Angell, S. Sivarajan, Glass transition, Reference Module in Materials Science and Materials Engineering, Elsevier, 2017, <https://doi.org/10.1016/B978-0-12-803581-8.03155-6>. <http://www.sciencedirect.com/science/article/pii/B9780128035818031556>
- [33] R. Kerner, M. Micoulaut, On the glass transition temperature in covalent glasses, *J. Non Cryst. Solids* 210 (2) (1997) 298–305, [https://doi.org/10.1016/S0022-3093\(96\)00678-3](https://doi.org/10.1016/S0022-3093(96)00678-3). <http://www.sciencedirect.com/science/article/pii/S0022309396006783>
- [34] R. Kerner, G.G. Naumis, Stochastic matrix description of the glass transition, *J. Phys.* 12 (8) (2000) 1641–1648, <https://doi.org/10.1088/0953-8984/12/8/306>.
- [35] G.G. Naumis, Variation of the glass transition temperature with rigidity and chemical composition, *Phys. Rev. B* 73 (2006) 172202, <https://doi.org/10.1103/PhysRevB.73.172202>.
- [36] M. Micoulaut, G.G. Naumis, Glass transition temperature variation, cross-linking and structure in network glasses: a stochastic approach, *Europhys. Lett.* 47 (5) (1999) 568–574, <https://doi.org/10.1209/epl/i1999-00427-7>.
- [37] S. Sen, J.K. Mason, Topological constraint theory for network glasses and glass-forming liquids: a rigid polytope approach, *Front. Mater.* 6 (2019) 213, <https://doi.org/10.3389/fmats.2019.00213>. <https://www.frontiersin.org/article/10.3389/fmats.2019.00213>
- [38] D. Simatos, G. Blond, G. Roudaut, D. Champion, J. Perez, A.L. Faivre, Influence of heating and cooling rates on the glass transition temperature and the fragility parameter of sorbitol and fructose as measured by dsc, *J. Therm. Anal.* 47 (5) (1996) 1419–1436, <https://doi.org/10.1007/BF01992837>.
- [39] C.T. Moynihan, A.J. Eastale, J. Wilder, J. Tucker, Dependence of the glass transition temperature on heating and cooling rate, *J. Phys. Chem.* 78 (26) (1974) 2673–2677, <https://doi.org/10.1021/j100619a008>.
- [40] G.G. Naumis, Simple solvable energy-landscape model that shows a thermodynamic phase transition and a glass transition, *Phys. Rev. E* 85 (2012) 061505, <https://doi.org/10.1103/PhysRevE.85.061505>.
- [41] J.Q. Toledo-Marn, G.G. Naumis, Short time dynamics determine glass forming ability in a glass transition two-level model: a stochastic approach using kramers-escape formula, *J. Chem. Phys.* 146 (9) (2017) 094506, <https://doi.org/10.1063/1.4977517>.
- [42] J.Q. Toledo-Marn, I.P. Castillo, G.G. Naumis, Minimal cooling speed for glass transition in a simple solvable energy landscape model, *Physica A* 451 (2016) 227–236, <https://doi.org/10.1016/j.physa.2016.01.064>. <http://www.sciencedirect.com/science/article/pii/S0378437116001187>
- [43] L. Bonilla, F. Padilla, F. Ritort, Aging in the linear harmonic oscillator, *Physica A*

- 250 (1–4) (1998) 315–326. <http://www.sciencedirect.com/science/article/pii/S0378437197005475>
- [44] A. Garriga, F. Ritort, Mode-dependent nonequilibrium temperature in aging systems, *Phys. Rev. E* 72 (2005) 031505, <https://doi.org/10.1103/PhysRevE.72.031505>.
- [45] M. Micoulaut, Linking rigidity transitions with enthalpic changes at the glass transition and fragility: insight from a simple oscillator model, *J. Phys.* 22 (28) (2010) 285101, <https://doi.org/10.1088/0953-8984/22/28/285101>.
- [46] X. Guo, J.C. Mauro, D.C. Allan, Y. Yue, On the frequency correction in temperature-modulated differential scanning calorimetry of the glass transition, *J. Non Cryst. Solids* 358 (14) (2012) 1710–1715, <https://doi.org/10.1016/j.jnoncrsol.2012.05.006>.
- [47] G. Naumis, J. Phillips, Diffusion of knowledge and globalization in the web of twentieth century science, *Physica A* 391 (15) (2012) 3995–4003, <https://doi.org/10.1016/j.physa.2012.02.005>.
- [48] N. Metropolis, A.W. Rosenbluth, M.N. Rosenbluth, A.H. Teller, E. Teller, Equation of state calculations by fast computing machines, *J. Chem. Phys.* 21 (6) (1953) 1087–1092, <https://doi.org/10.1063/1.1699114>.
- [49] P.K. Gupta, J.C. Mauro, Composition dependence of glass transition temperature and fragility. i. a topological model incorporating temperature-dependent constraints, *J. Chem. Phys.* 130 (9) (2009) 094503, <https://doi.org/10.1063/1.3077168>.
- [50] J.C. Mauro, P.K. Gupta, R.J. Loucks, Composition dependence of glass transition temperature and fragility. ii. a topological model of alkali borate liquids, *J. Chem. Phys.* 130 (23) (2009) 234503, <https://doi.org/10.1063/1.3152432>.
- [51] J.C. Mauro, R.J. Loucks, Selenium glass transition: a model based on the enthalpy landscape approach and nonequilibrium statistical mechanics, *Phys. Rev. B* 76 (2007) 174202, <https://doi.org/10.1103/PhysRevB.76.174202>.
- [52] J.C. Mauro, Y. Yue, A.J. Ellison, P.K. Gupta, D.C. Allan, Viscosity of glass-forming liquids, *Proc. Natl. Acad. Sci.* 106 (47) (2009) 19780–19784, <https://doi.org/10.1073/pnas.0911705106>.
- [53] J.C. Mauro, D.C. Allan, M. Potuzak, Nonequilibrium viscosity of glass, *Phys. Rev. B* 80 (2009) 094204, <https://doi.org/10.1103/PhysRevB.80.094204>.
- [54] M.M. Smedskjaer, J.C. Mauro, Y. Yue, Ionic diffusion and the topological origin of fragility in silicate glasses, *J. Chem. Phys.* 131 (24) (2009) 244514, <https://doi.org/10.1063/1.3276285>.
- [55] J.C. Mauro, C.S. Philip, D.J. Vaughn, M.S. Pambianchi, Glass science in the united states: current status and future directions, *Int. J. Appl. Glass Sci.* 5 (1) (2014) 2–15.